PROCEEDINGS OF SCIENCE

Simulation study of pulse height difference between pixel patterns of X-ray CCDs onboard the XRISM satellite

Yuma AOKI,[a,*] Kumiko K. NOBUKAWA, Yamato ITO,[a] Masayoshi NOBUKAWA,[b] Yoshiaki KANEMARU, Keitaro MIYAZAKI, Kohei KUSUNOKI, Koji MORI,[c] Tomokage YONEYAMA,[d] Tsubasa TAMBA,[e] Hiroshi TOMIDA,[f] Hiroshi NAKAJIMA,[g] Hironori MATSUMOTO, Hirofumi NODA, Kiyoshi HAYASHIDA,[h] Takeshi G. TSURU, Hiroyuki UCHIDA,[i] Takaaki TANAKA, Hiromasa SUZUKI,[j] Tessei YOSHIDA,[f] Hiroshi MURAKAMI,[l] Makoto YAMAUCHI, Isamu HATSUKADE,[c] Kouichi HAGINO,[e] Takayoshi KOHMURA,[o] Shogo B. Kobayashi,[t] Junko S. HIRAGA,[p] Hideki UCHIYAMA,[q] Kazutaka YAMAOKA,[r] Masanobu OZAKI,[s] Tadayasu DOTANI,[d] Hiroshi TSUNEMI[h] and XRISM/Xtend team

[a] *Department of Physics, Kindai University, 3-4-1 Kowakae, Higashi-Osaka, Osaka 577-8502*

[b] *Faculty of Education, Nara University of Education, Takabatake-cho, Nara, Nara 630-8528*

[c] *Faculty of Engineering, University of Miyazaki, 1-1 Gakuen Kibanadai Nishi, Miyazaki 889-2192*

[d] *Japan Aerospace Exploration Agency, Institute of Space and Astronautical Science, 3-1-1 Yoshino-dai, Chuo-ku, Sagamihara, Kanagawa 252-5210*

[e] *Department of Physics, University of Tokyo, 7-3-1 Hongo, Bunkyo, Tokyo 113-0033*

[f] *Japan Aerospace Exploration Agency, Institute of Space and Astronautical Science, 2-1-1, Sengen, Tsukuba, Ibaraki 305-8505*

[g] *College of Science and Engineering, Kanto Gakuin University, 1-50-1 Mutsuurahigashi, Kanazawa-ku, Yokohama, Kanagawa 236-8501*

[h] *Department of Earth and Space Science, Osaka University, 1-1 Machikaneyama-cho, Toyonaka, Osaka 560-0043*

[i] *Department of Physics, Kyoto University, Kitashirakawa Oiwake-cho, Sakyo, Kyoto, Kyoto 606-8502*

[j] *Department of Physics, Konan University, 8-9-1 Okamoto, Higashinada, Kobe, Hyogo 658-8501*

[l] *Faculty of Liberal Arts, Tohoku Gakuin University, 2-1-1 Tenjinzawa, Izumi-ku, Sendai, Miyagi 981-3193*

[o] *Department of Physics, Tokyo University of Science, 2641 Yamazaki, Noda, Chiba 270-8510*

[p] *Department of Physics, Kwansei Gakuin University, 2-1 Gakuen, Sanda, Hyogo 669-1337*

[q] *Science Education, Faculty of Education, Shizuoka University, 836 Ohya, Suruga-ku, Shizuoka 422-8529*

[r] *Department of Physics, Nagoya University, Furo-cho, Chikusa-ku, Nagoya, Aichi 464-8602*

[s] *National Institutes of Natural Sciences National Astronomical Observatory of Japan, 2-21-1 Osawa, Mitaka, Tokyo 181-8588*

[t] *Department of Physics, Tokyo University of Science, 1-3, Kagurazaka, Sinjuku-ku, Tokyo 162-0825*

E-mail: messier.aoki@kindai.ac.jp

*Speaker

© Copyright owned by the author(s) under the terms of the Creative Commons Attribution-NonCommercial-NoDerivatives 4.0 International License (CC BY-NC-ND 4.0).

PoS(Pixel2022)036

We have developed a soft X-ray telescope system Xtend onboard Japan's new X-ray astronomical satellite XRISM. Xtend employs X-ray CCDs, which have basically the same design as those used in the previous X-ray astronomical satellite Hitomi. Monochromatic X-ray line spectra of the CCDs onboard Hitomi showed offsets of centroids between different pixel patterns or different good grades; the spectral centroids of charge-sharing events are higher than those of single-pixel events. The spectral offset, which we call "Goffset", can cause large uncertainties in X-ray energy determination accuracy. In this paper, confirming the CCDs onboard XRISM also have Goffset, we performed a simulation study that takes into account the two factors; charge sharing and readout noise. Goffset of the flight model CCD is successfully reproduced by the simulation with a certain readout noise. We investigate how charge sharing and readout noise cause Goffset based on the simulation results.

PoS(Pixel2022)036

10th International Workshop on Semiconductor Pixel Detectors for Particles and Imaging,
12-16 December 2022
Santa Fe, New Mexico, USA

1. Introduction

The X-Ray Imaging and Spectroscopy Mission (XRISM) is Japan's seventh X-ray astronomy mission [1], and its launch is scheduled for the Japanese fiscal year 2023. XRISM is equipped with two instruments, Resolve [2] and Xtend [3], each of which consists of an X-ray Mirror Assembly (XMA) and a focal plane detector with a focal length of 5.6 m. The focal plane detector of Resolve is an X-ray microcalorimeter, and will offer non-dispersive, high-resolution X-ray spectroscopy (ΔE ~7 eV@6 keV), but with a narrow field of view (only $2.9' \times 2.9'$). On the other hand, the focal plane detector of Xtend is the Soft X-ray Imager (SXI), an X-ray CCD camera with typical energy resolution for CCDs (ΔE ~200 eV@6 keV). A characteristic of Xtend is a wide field of view of $38' \times 38'$, which makes Xtend complementary to Resolve in imaging.

The SXI has basically the same design as the one onboard Hitomi. Four CCDs are arranged in a 2×2 grid and can be cooled down to -120°C with a single-stage Stirling cooler. The SXI used the P-channel back-illuminated type CCDs Pch-NeXT4A manufactured by Hamamatsu Photonics K.K. The SXI CCDs are fully depleted in a depletion layer of 200 μm, which enables the SXI to cover an energy range of up to 12 keV. Specifications of the SXI CCDs are summarized in table 1, and more details are reported in Ref.[3]. Each CCD has four readout nodes. Halves of the imaging area are read out by the two of them and processed by the individual circuits so that we obtain two "segment" images per CCD in every frame cycle.

Table 1: Specifications of the XRISM CCDs

Imaging area	30.72 mm × 30.72 mm
Pixel size	24 μm × 24 μm (after on-chip 2 × 2 binning)
Pixel number	640 × 640 pixels/CCD (after on-chip 2 × 2 binning)
Depletion layer	200 μm
Energy resolution	≤ 200 eV @5.9 keV
Energy range	0.4 – 13 keV

When an X-ray photon enters an X-ray CCD and is photo-absorbed in the depletion region, electron-hole pairs (called a "charge cloud") are created in a narrow region. The produced charges drift to the potential well formed below the electrodes to be collected. Ideally, the charges are all collected by a single pixel, but in practice, the charges often spread into neighboring pixels, resulting in a multi-pixel event. After the charges are collected, the transfer occurs between the potential wells. The incident X-ray energy is determined by measurement of the amount of the charges.

The distinction between X-ray-induced and (non-X-ray) particle-induced events is critical for X-ray observations because a charged particle generates the electron-hole pairs along its track in the CCD. The SXI adopts the Grade method, where X-ray-induced events are distinguished from particle-induced ones by pixel patterns or "Grade"; charge clouds produced by an X-ray photon are more likely to be confined than those produced by particles. The Grade method has been employed first in ASCA, and then in other CCD detectors of subsequent X-ray satellites. Events classified into Grade 0, 2, 3, 4, and 6 (good Grades) are considered to be induced by X-rays, while other Grades (bad Grades) are considered to be non-X-ray events. The bigger Grade number indicates that the event has spread charges over more pixels. An event where charges are concentrated in a single

PoS(Pixel2022)036

pixel is classified as Grade 0 whereas the one where charges are spread over three or four pixels falls into Grade 6. A neighboring pixel whose pulse height is above the split threshold is assumed to share charges with the event's center pixel.

A spectrum of events with the same energy in each good grade ideally should coincide with each other. However, the CCDs onboard Hitomi showed offsets of centroids between the good Grade spectra. The centroids of multiple-pixel charge-sharing event spectra are higher than that of single-pixel events; the more pixels share the charge, the larger offsets of spectral centroids. We call the spectral offsets between good Grades, "Goffset". It can cause large uncertainties in X-ray energy determination accuracy, but its cause has been unclear. In this paper, we evaluated Goffset with the flight model of the SXI CCDs and found that their spectra show energy-dependent Goffset. We also investigated the cause of Goffset through a simple pulse height simulation.

2. Goffset of the flight model XRISM CCDs

An on-ground calibration was conducted in April 2021 with the flight model CCDs installed in a laboratory system. The CCDs were irradiated with monochromatic X-rays produced by radioisotopes (^{55}Fe and ^{241}Am) and an X-ray generator. Three targets for the X-ray generator were used: LiF, Al, and SiO_2. The detail of the laboratory system and X-ray generator is described in Ref.[6]. We used the data of the segment "CCD2AB" since the segment exhibits the highest charge transfer efficiency and energy resolution among the flight model CCDs.

We focus on the data of four characteristic X-rays: F Kα (E = 0.677 keV), Al Kα (E = 1.487 keV), Si Kα (E = 1.740 keV), and Mn Kα (E = 5.895 keV). Figure 1 shows F Kα and Mn Kα spectra of the Grade 0 and Grade 6 events. In both panels, we see an offset of the centroids of the Grade 0 and Grade 6 spectra and confirm that the XRISM CCD has Goffset. We obtained the energy dependence of Goffset as shown in figure 2(a). Here, PHA[Gn] denotes the centroid of Grade n spectrum, and Goffset is defined as PHA[G6]−PHA[Gn] ($n = 0, 2, 3, 4$). Goffset of Grade 0 (PHA[G6]−PHA[G0]) is $\sim$ 1% of PHA[G6] in the high energy of $\sim$ 1000 ch ($\sim$ 6 keV) while in the low-energy end of $\sim$ 120 ch ($\sim$ 0.7 keV), Goffset sharply increases up to 11 % of PHA[G6]. We also analyzed the segment of CCD2CD for comparison (figure 2b) and found that its Goffset is different from that of CCD2AB especially in the low-energy end, despite the identical CCD chip.

3. Simulation and results

One possible cause of Goffset is charge sharing. When charges are shared with several pixels, and a pulse height in some pixels is lower than the split threshold, their pulse height is not counted as a signal. The more pixels that have a lower pulse height than the split threshold result in a more uncounted pulse height. Grade 0 events are expected to most in the case.

The other factor of Goffset can be readout noise, which is indicated by the fact that Goffset is different between the segments in the identical CCD chip (figure 2b). The sharp increase of Goffset in the low-energy end, where the signal-to-noise ratio is lower, also implies noise's contribution. We perform a simple simulation that takes into account the two factors to evaluate their contribution to Goffset.

PoS(Pixel2022)036

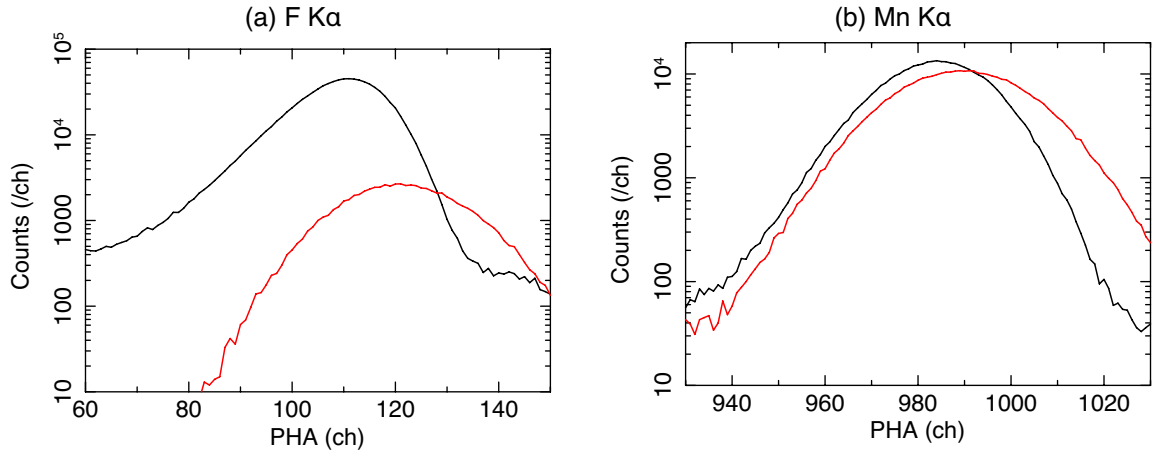

Figure 1: (a) F Kα spectra of the segment CCD2AB of the XRISM CCDs. The black and red data represent the spectra of Grade 0 events and Grade 6 events. (b) Same as (a), but for the Mn Kα spectra.

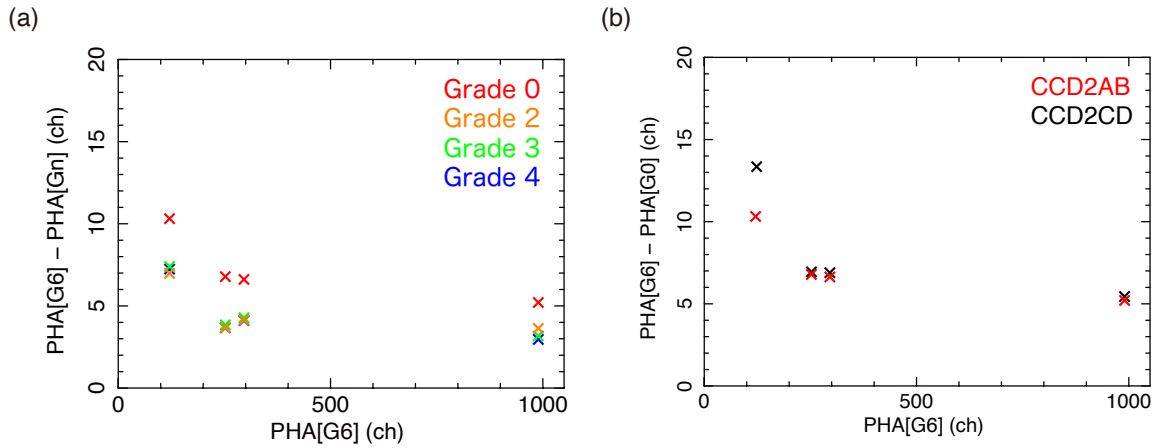

Figure 2: (a) Goffsets for Grade 0, 2, 3, 4 of the segment CCD2AB of the XRISM CCDs; namely the centroid deferences between the line spectra of Grade 6 and Grade n events ($n = 0, 2, 3, 4$). (b) Comparison of Goffsets for Grade 0 of CCD2AB (red) and CCD2CD (black).

The simulation procedure is as follows. We assume a charge cloud collected in a potential well; the cloud has a density of 2-dimension Gaussian with standard deviation σ. The number of charges in the cloud is expressed by a given initial pulse height (denoted by PHA_0) and has Fano fluctuations. Fano factor for Si has been empirically obtained to be $F = 0.115$ and we adopt this value. The charge cloud is randomly placed on a pixel, collected in the single pixel or shared by neighboring pixels, and anyway read out as a pulse height of each pixel (denoted by PH). PH is subject to random readout noise, which is assumed to obey a Gaussian distribution with a centroid of 0 and a standard deviation of N. According to the final PH distribution including both the signal charges and noise, Grade is determined for each event, and PH of each surrounding 3×3 pixels above the split threshold is accumulated into the total pulse height of the event (denoted by PHA). The above procedure was tried 100,000 times to produce a spectrum for each Grade. The individual spectra were fitted with Gaussian to obtain PHA[Gn] ($n = 0, 2, 3, 4, 6$). Finally, simulated Goffset

PoS(Pixel2022)036

is obtained by PHA[G6]−PHA[Gn].

The initial pulse height PHA_0 was varied from 100 ch to 1000 ch whereas the standard deviations N of the random noise were varied from 0 ch to 10 ch. The charge cloud size σ is not a priori clear. We simulated Grade branching ratio with various σ values both for $\mathrm{PHA}_{=}120$ ch and 1000 ch, which correspond to F Kα and Mn Kα lines, respectively. The actual Grade branching ratio of the segment CCD2AB for both F Kα and Mn Kα lines were well reproduced by σ =0.11 pixel, and thus we hereafter fix σ =0.11 pixel regardless of the incident X-ray energy. The simulation parameters are summarized in table 2.

Table 2: Parameters of simulation

Parameter	Value
Fano factor F	0.115
Standard deviation of charge cloud distribution σ	0.11 pixel
Initial pulse height PHA_0	100–1000 ch
Standard deviation of noise N	0–10 ch
Split threshold	15 ch

Figure 3 displays the simulated spectra of the Grade 0 and Grade 6 events with PHA_0 = 120 and 1000 ch. The two cases of N = 0 ch and N = 6 ch are compared. In the former case, PHA[G6] is almost equal to PHA_0, which means that almost all shared charges are counted in PHA, whereas PHA[G0] is lower than PHA_0. As for the spectra of N = 6 ch, PHA[G0] is still lower than PHA_0, but PHA[G6] exceeds PHA_0. Notably, the simulated spectra of N = 6 ch have a very similar shape to the ones of the flight model CCD (figure 1).

The simulated Goffset for Grade 0 (PHA[G6]−PHA[G0]) is shown in figure 4 for N = 0, 2, 4, 6, 8 ch. We adopt PHA[G6] for the horizontal axis to compare with the actual data. The N = 0 case indicates Goffset of a few ch for any PHA[G6]. For low N values (< 4 ch), Goffset slightly increases as PHA[G6] does. As N increases, Goffset rapidly increases especially on the low-energy side. The Goffset of CCD2AB, which is denoted by the cross marks, is well reproduced by the simulation result of N = 6 ch within 1 ch accuracy. We confirm that the simulated Goffset for Grade 2, 3, and 4 are also explained by the simulation of N = 6 ch as shown in figure 5.

4. Discussion

We conducted the simple Goffset simulation incorporating the charge-sharing effect and noise addition and found that Goffset increases as noise does, especially on the low-energy side. Goffset of the flight model CCD is explained by the simulation result of N = 6 ch. Here we discuss how Goffset is induced by charge sharing and readout noise.

The charge-sharing effect would be dominant for low noise (N < 4 ch). The simulated spectra of N = 0 ch (figures 3a and 3b) indicate that PHA[G6] is almost equal to PHA_0 whereas PHA[G0] is less than PHA_0 by a few ch, which results in Goffset. In the Grade 0 events, PH of each charge-sharing pixel less than the split threshold is not counted in PHA so that PHA[G0] becomes below PHA_0. Sharing charges increase as PHA or a number of charges does, and thus Goffset slightly increases with PHA.

PoS(Pixel2022)036

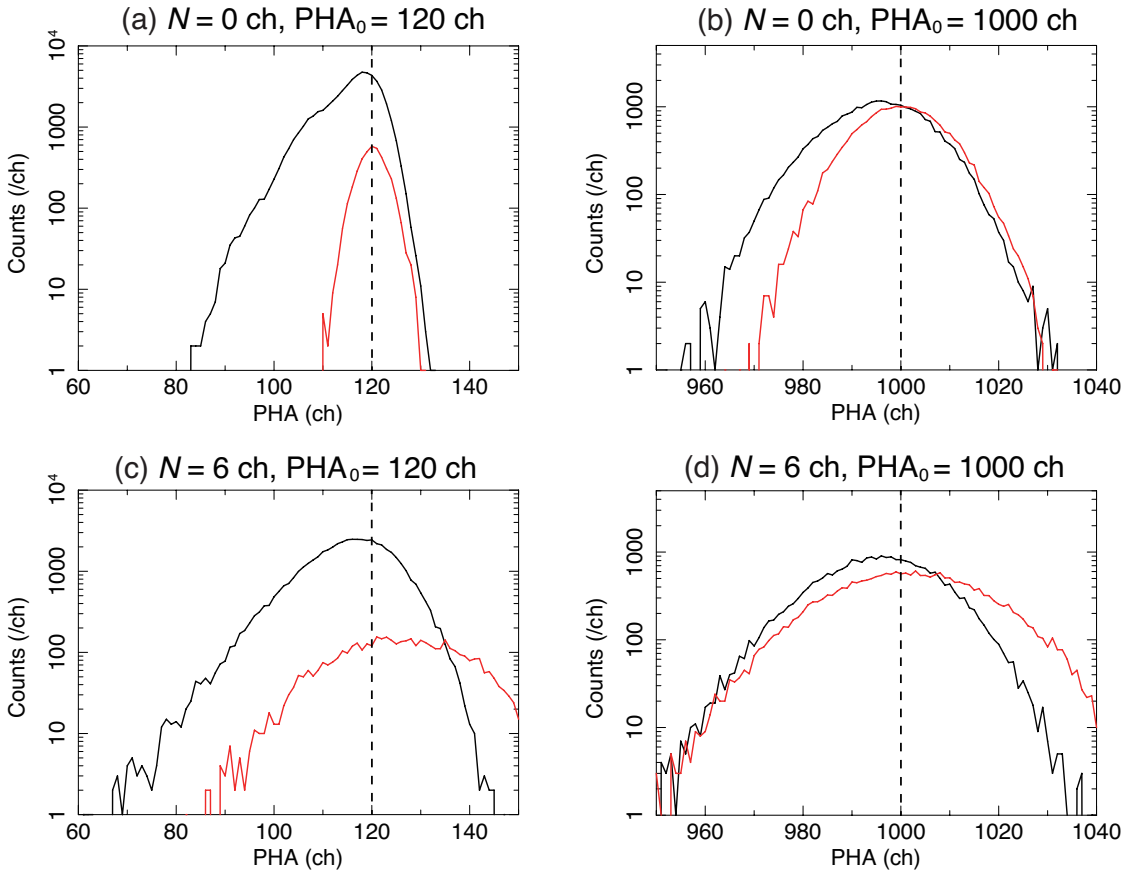

Figure 3: (Top) Simulated spectra of Grade 0 (black) and Grade 6 (red) with N = 0 ch for PHA_0=120 ch (a) and PHA_0=1000 ch (b). The dashed line represents PHA_0. (Bottom) Same as the top, but those with N = 6 ch.

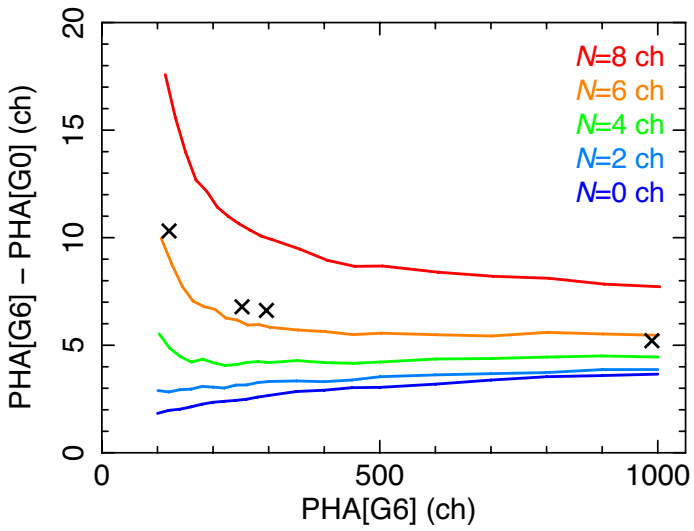

Figure 4: Simulated Goffset of Grade 0 for N = 0, 2, 4, 6, 8 ch overlapped by the actual Goffset of the flight model CCD (segment CCD2AB; see figure 2a) denoted by the cross marks.

PoS(Pixel2022)036

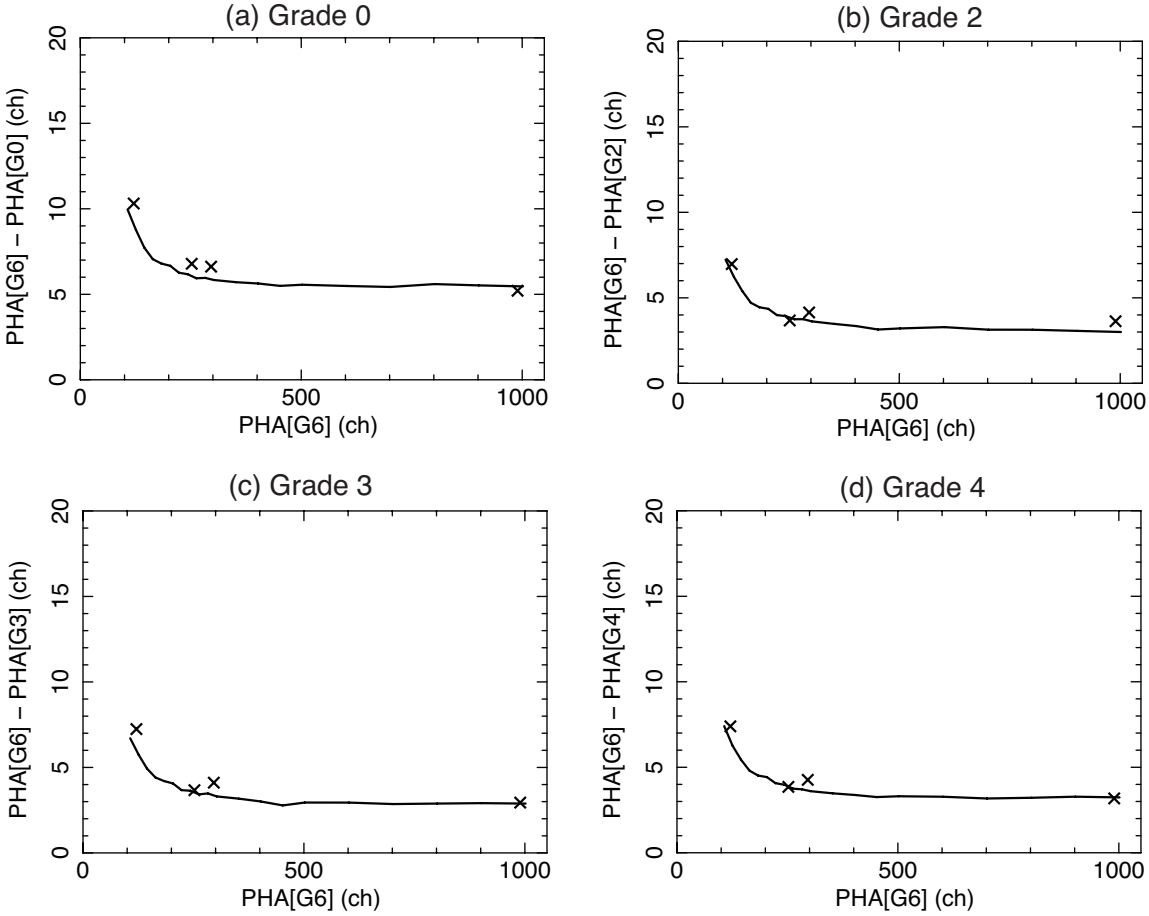

Figure 5: Filled circles represent simulated Goffset of Grade 0 (a), 2 (b), 3 (c), 4 (d) for $N = 6$ ch and $\sigma = 0.11$ pixel. The cross marks denote the measured Goffsets of the segment of CCD2AB.

Goffset increases systematically as noise increases at any PHA_0. The simulated spectra of $N = 6$ ch (figures 3c and 3d) show that PHA[G0] is only slightly less than PHA_0 and almost the same between $N = 0$ ch and $N = 6$ ch whereas PHA[G6] increases with noise to exceed PHA_0, which results in higher Goffset. Let's consider an event that is originally Grade 0 when $N = 0$ ch. The added noise is assumed to follow the Gaussian distribution and can fluctuate positively or negatively. If noise in the surrounding pixels fluctuates negatively, the event is still classified as Grade 0, and the accumulated PHA remains almost the same as the original one. This contrasts the increase in PHA and Grade modification when the noise fluctuates positively; the Grade 0 event would be identified as higher Grade. For Grades 2, 3, and 4 events, noise can modify Grade from the original. There are two cases; (1) original charges are put within a single pixel but the event is classified as a higher Grade due to the addition of positively fluctuating noise, and (2) original charges are shared by more pixels but the event is classified as a lower Grade due to the addition of negatively fluctuating noise. Thus, Grade 0 events are biased to contain events with negatively fluctuating noise, and Grade 6 events are biased to contain events with positively fluctuating noise.

Figure 6, which shows simulated Grade branching ratio of $\mathrm{PHA}_0 = 120$ ch and $\mathrm{PHA}_0 = 1000$ ch for $N = 0$ ch and $N = 6$ ch, also supports the above picture. The measured Grade branching ratio

PoS(Pixel2022)036

is overlapped with the figure and we confirm that the measured one is generally consistent with the simulation result of $N = 6$ ch. For $\mathrm{PHA}_0 = 120$ ch, the Grade 0 events are the majority and the ratio of Grade 6 is only ∼5%. On the other hand, for $\mathrm{PHA}_0 = 1000$ ch, the ratio of Grade 0 decreases to ∼25% and that of Grade 6 increases to ∼20%. This is because the amount of charges shared by the neighboring pixels is small for the low PHA_0 and below the split threshold in most cases. By adding noise, the ratio of Grade 0 decreases because some originally Grade 0 events are classified as multiple-pixel events or higher Grade, due to positively fluctuated noise in the surrounding pixels. Indeed, some originally higher Grade events are modified to Grade 0 events due to negatively fluctuated noise, but their frequency is smaller than the former. The ratios of Grade 2, 3, and 4 appear to be not affected well by noise because Grade modifications due to positively and negatively fluctuated noise cancel each other out. Some events whose Grade is originally less than 6 are modified to Grade 6 due to positively fluctuating noise, which increases the Grade 6 ratio in $N = 6$ ch.

The problem is that Goffset increases rapidly on the low-energy side as noise does as shown in figure 4. Figures 3(c) and 3(d) show that Goffset increase on the low-energy side is not because the difference between PHA[G0] and PHA_0 grows, but because the difference between PHA[G6] and PHA_0 does at the low energy. This would be due to two factors. (1) For high PHA_0, missing charges and positively fluctuated noise partially cancel each other out, and therefore the difference between PHA_0 (or PHA[G6]) and PHA[G0] does not grow so much. However, for low PHA_0, the added positively fluctuated noise is directly counted in PHA, so the difference between PHA_0 and PHA[G6] grows with noise. (2) The ratio of Grade 6 is lower for lower PHA_0. The proportion of the Grade 6 events that are originally lower Grade ones but modified to Grade 6 due to the positively fluctuated noise is relatively higher for low PHA_0.

5. Conclusion

We investigated differences in spectral centroids between good Grades, and Goffset, in the Xtend CCDs onboard XRISM, and confirmed that they show Goffset as in Hitomi. We assumed that there were two factors contributing to Goffset; charge sharing and noise. To examine this assumption, we performed the simple simulation and obtained the following results:

1. Our simulation with $N = 6$ ch reproduced Goffset of the flight model CCD as well as the measured spectrum of the good Grades.

2. Without noise ($N = 0$), there is a positive correlation between PHA and Goffset. This would be due to the effect of charge sharing. The higher PHA_0 makes more missing charges or higher missing PH below the split threshold in the surrounding pixels.

3. When noise increased, Goffset becomes larger systematically. This is because Grade 0 events are biased to contain events with negatively fluctuating noise whereas Grade 6 events are biased to contain events with positively fluctuating noise. Thus PHA[G6] increases with noise to exceed PHA_0 whereas PHA[G0] is almost the same at any noise.

4. Goffset rapidly increases especially in low PHA_0. This would be due to the following reason. When a positive fluctuating noise is added to a Grade 0 event and thus Grade is modified to a

PoS(Pixel2022)036

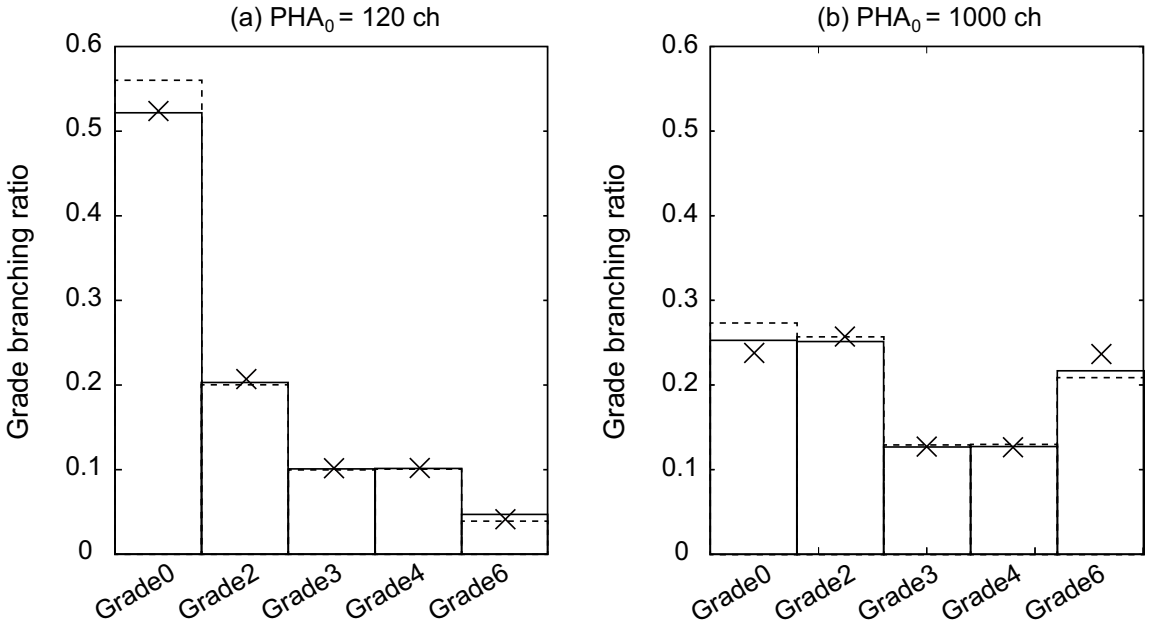

Figure 6: Simulated Grade branching ratio of Grade 0, 2, 3, 4, and 6 with N = 0 ch (dashed lines) and N = 6 ch (solid lines) for PHA=120 ch (a) and 1000 ch (b). The cross marks of each panel denote the Grade branching ratios for the F Kα (a) and Mn Kα lines (b) of the flight model CCD.

higher one, the noise and the missing PH below the split threshold partially cancel each other out, especially in high PHA$_0$. On the other hand, in low PHA$_0$, the added positive noise is directly counted in PHA. Also, the low ratio of Grade 6 in low PHA$_0$ makes the relatively high proportion of Grade 6 events that are originally lower Grade events but modified to Grade 6 with the positive noise addition.

This study successfully reproduced Goffset by the simulation that takes charge sharing and noise into account. It is expected that an on-orbit noise will have different values from that on the ground test. This simulation will assist Goffset correction in the on-orbit calibration with limited data.

References

[1] M. Tashiro et al. *Status of x-ray imaging and spectroscopy mission (XRISM)*, 2020, Proc. SPIE 11444, 1144422.

[2] Y. Ishisaki et al. *Resolve Instrument on X-ray Astronomy Recovery Mission (XARM)*, 2018, Journal of Low Temperature Physics 193, 9912013-995.

[3] K. Mori et al. *Xtend, the soft x-ray imaging telescope for the X-Ray Imaging and Spectroscopy Mission (XRISM)*, 2022, Proc. SPIE 12181, 121811T.

[4] H. Nakajima et al. *In-orbit performance of the soft X-ray imaging system aboard Hitomi (ASTRO-H)*, 2018, PASJ 70, 21.

PoS(Pixel2022)036

[5] T. Tamba et al. *Simulation-based spectral analysis of X-ray CCD data affected by photon pile-up*, 2022, PASJ 74, 364–383.

[6] T. Yoneyama et al. *Screening and selection of XRISM/Xtend flight model CCD*, 2020, NIMA 985, 164676.

PoS(Pixel2022)036